3. STRUCTURAL EVALUATION OF DEPLOYABLE AERODYNAMIC SPIKE BOOMS

By B. J. Richter*

ABSTRACT

An extendable boom consisting of a series of telescopic cylindrical tube segments and overlapping lock joints is being developed for use as an aerodynamic spike mounted atop a missile. Two candidate design concepts differing mainly in the particular overlapping lock joint designs are currently undergoing a combined analytical/experimental evaluation. Some of the results of this evaluation are presented in this paper.

INTRODUCTION

In order to increase its range by reducing aerodynamic drag, a missile is to be flown with a completely mechanical and self-contained deployable aerodynamic nose spike system. A typical aerodynamic flow pattern induced by the aerospike mounted atop a missile's nose fairing is illustrated in figure 1. The worst expected loading condition for the deployed spike boom results from aerodynamically induced static and dynamic pressures and is statically equivalent to a 2300 lb compressive axial load and a 360 lb lateral load both applied at the extended boom tip. The aerospike system consists of a series of telescopic cylindrical boom segments, an inertial initiator, and a gas generator, which are housed in the stowed configuration inside a case mounted in the missile nose fairing. In the extended position the telescopic boom segments obtain their axial and lateral rigidity from a series of overlapping lock joints.

Two extendable boom design concepts are currently being evaluated and differs from each other mainly in the design of the overlapping lock joints employed. Each concept is being evaluated both analytically and experimentally and after the evaluation is complete, one of the design concepts will be chosen as baseline for the missile. The progress on some of the structural aspects of the current analytical/experimental investigation of these two extendable boom design concepts is the subject of this paper.

STRUCTURAL DESIGN REQUIREMENTS

The following lists some of the more important structural design requirements which the aerospike boom must meet.

1. The extended length must be 50 ± 1 inch.

2. The stowed length must be ≤11.5 inches.

---

*Lockheed Missiles & Space Company, Inc., Sunnyvale, California.

3. The extended boom must be capable of supporting a 2300 lb compressive axial load and a 360 lb lateral load both applied at the boom tip.

4. The deployment process must minimize axial impact stopping loads imposed upon the housing/nose cap structure.

5. The overlapping joints shall act to laterally align the individual boom segment centerlines of the fully extended aerospike within 0.5 inch of the missile centerline.

6. The first cantilevered lateral bending frequency of the fully extended and locked aerospike boom with a 2 lb tip disc shall be ≥35 Hz.

7. The entire deployment and locking process shall take place within 1 second after the inertial initiator ignites the gas generator.

MECHANISM OPERATION

The deployable aerodynamic spike system consists of a series of N telescopic boom segments, an inertial initiator, a gas generator, and a housing which is attached inside the missile nose fairing. This system is illustrated schematically in the stowed configuration in figure 2a. After the missile is launched the inertial initiator senses an appropriate missile acceleration profile and ignites a gas generator. The gases produce a history of internal pressure which initially acts to break a hold-down bolt. The gas pressure then acts on the individual telescopic boom segments S_i and accelerates them into an extended and locked configuration as illustrated in figure 2b. The positioning and the locking of the boom segments are accomplished by a series of overlapping lock joints J_i. The positioning must be such that the centerlines of the individual segments S_i be laterally aligned within specified tolerance limits with the missile centerline, and that the final extended length L = 50 inches.

After the aerospike boom has been extended and locked into place, it is subjected to a history of aerodynamically induced heating and loading. The joints J_i are then required to transfer loads (i.e., axial loads, bending moments, and shears) from one segment to the next. As an example, two ways in which the bending moment M shown in figure 3a can be transferred from segment S_{i+1} across joint J_{i+1} to segment S_i are illustrated in figures 3b and 3c. In these figures e represents the axial engagement or joint overlap distance. The first way is illustrated in figure 3b. In this case the moment is reacted by a couple cF. In the second case, shown in figure 3c, the moment M is reacted by the couple cP. The couple forces F are the resultants of surface stresses distributed in the joint region which act parallel to the tube centerline. The couple forces P are the resultants of surface stresses distributed in the joint region which act perpendicular to the tube centerline. There also exists a third way which is simply a combination of the above two ways.

If the deployed aerospike boom segments and joints were not a mechanism (e.g., if the segments could be welded together), then a moment M would be reacted as in classical beam bending theory. The bending stresses σ would be given by

$$\sigma = M/(\pi R^2 t),\qquad(1)$$

32

where R and t are the tube radius and thickness, respectively. For $\sigma = 100,000$ psi, $R = 2$ inches, and $t = 0.1$ inch the allowable theoretical bending moment capability M_A of the boom is found, using (1), to be

$$M_A = 125,000 \text{ in.-lb} \tag{2}$$

Because the aerospike is a mechanism, however, the joint design produces actual allowable bending moment capabilities far below the theoretical value given by (2). These reduced bending allowables will be discussed in more detail later in this paper.

One important parameter which determines how a particular joint functions is the engagement distance e. This parameter is geometrically related to the three parameters L, ℓ, and N which are defined in figure 2. Since L and ℓ are fixed by the requirements such that $L = 50$ inches and $\ell = 11.5$ inches, a unique relation exists between e and N. From geometric considerations (fig. 2) this relation is found to be

$$e = 11.5'' - 50''/N, \tag{3}$$

with the further requirements that $0 < e < 11.5$ inches. Hence, the smallest number of segments that will satisfy (3) is $N = 5$. This corresponds to an $e = 1.5$ inches. An $N = 6$ corresponds to an $e = 3.2$ inches. These two cases form the geometric basis of the two design concepts which are discussed in this paper.

Design concept I employs five steel cylindrical tube segments with tube radii varying from 2.14 to 1.50 inches and corresponding tube wall thickness varying from 0.141 to 0.078 inch. The manner in which joint J_{i+1} locks together segments S_i and S_{i+1} is illustrated schematically in figure 4 (the angle β in fig. 4 is exaggerated and typically is about 1.5°). Segment S_{i+1} approaches the joint region J_{i+1} with a velocity v relative to S_i as shown in figure 4a. Surface AB of S_{i+1} initially encounters surface CD of S_i as shown in figure 4b. At this time the engagement is e_0. The two segments then swage together; the engagement e_0 decreases to e; and S_{i+1} comes to a halt relative to S_i. The two segments are then held together entirely by frictional stresses developed during the swaging process.

Design concept II employs six steel cylindrical tube segments with tube radii varying from 2.19 to 0.97 inches and corresponding tube wall thicknesses varying from 0.12 to 0.060 inch. The manner in which joint J_{i+1} locks together segments S_i and S_{i+1} is illustrated in figure 5. Segment S_{i+1} approaches the joint region with a velocity v relative to S_i as shown in figure 5a. Temporary relative stopping occurs when surface BC engages surface DE and surface HI engages surface JK. The radii of the various engaging surfaces are such that

$$r_{BC} - r_{DE} = r_{KJ} - r_{HI} = \Delta r \tag{4}$$

where Δr represents a radial interference. This interference fit causes frictional stresses to be generated in the contact regions which act to oppose the relative motion. The temporary motion again proceeds when the internal tube pressure builds up to a level high enough to overcome the frictional forces. Final joint locking occurs when surface AB impacts surface DF. At this time a ring of 24 locking fingers snaps into place along FG. The purpose of these locking fingers is to prevent any subsequent

33

relative motion in the opposite direction. This fully extended and locked joint configuration is illustrated in figure 5b.

EXPERIMENTAL INVESTIGATIONS

1. Axial engagement experiments were conducted on the two types of joint concepts. The geometries of the test specimens used for the types I and II joint concepts are shown respectively in figures 6a and 6b. Loading was applied with a hydraulic load cell. For the type I test specimen the force F required to reduce the initial engagement of 1.5 inches by amount δ is shown as the upper dashed curve in figure 7a. For increasing δ the applied force F increased from zero to a maximum of 10,000 lb and then fell off towards zero as δ approached 1.5 inches. For decreasing δ the experimentally determined $F(\delta)$ curve was found to be the lower dashed curve in figure 7a.

For the type II joint the applied force F required to partially engage the interference surfaces BC/DE and HI/JK (see fig. 5) ranged from zero up to a maximum of 2,000 lb. This force held constant at 2,000 lb as long as the surfaces BC/DE and HI/JK remained fully engaged.

2. An experiment was conducted on the design concept II joint configuration shown in figure 6b in order to investigate how a lateral force and bending moment are transferred across the joint. A hydraulically applied force P (see fig. 6b) was cycled between ±650 lb, and the lateral deflection Δ and the hoop strain ϵ indicated in figure 6b were monitored. The results for a load history 1-2-3-4-5-6-2 are shown in figures 7b and 7c. These figures indicate that this type of joint initially transfers the joint bending moment in the manner shown in figure 3b until $P = 300$ lb (path 1-2 in figs. 7b,c). At this load level the interference frictional shear stresses (which were generated when the two segments were initially pulled together) are overcome and slipping occurs. The increased bending moment caused by the loading in the 300 lb to 650 lb range (path 2-3 in fig. 7) is then carried across the joint in the manner shown in figure 3c. Repeated cycling retraces the path 2-3-4-5-6-2.

ANALYTICAL INVESTIGATIONS

1. The axial force required to reduce the initial engagement e_o by amount δ (see fig. 6a) can be computed by considering interference geometry, basic strength of materials, elastic behavior, and equilibrium of forces on the inner tube of figure 6a. This relation was found to be

$$F = k\delta(1 - \delta/e_o), \quad 0 \leq \delta \leq e_o \tag{5}$$

where

$$k = 2\pi t E e_o \tan \beta (\tan \beta \pm \mu)/R \tag{6}$$

34

with R and t being, respectively, the average tube radius and thickness. β is the cone half angle indicated in figure 4; μ is the interface coefficient of friction, and E is the material's Young's Modulus. The positive sign in (6) is for increasing δ while the negative sign is for decreasing δ. This relation is shown in figure 7a for $t = 0.0855$ inch, $R = 1.565$ inch, $E = 30,000,000$ psi, $e_o = 1.5$ inch, $\beta = 1.5$ degrees, and $\mu = 0.06$. The agreement of this rather simple formula with the experimental data is fairly good in view of the rather complex behavior of this joint.

2. A reasonable estimate of the load P at which slipping first occurs at point 2 (see figure 7b) can be obtained from elementary considerations as

$$P_{SLIP} = (F_e)(R + e)/(\pi h) \tag{7}$$

In this equation R is again the average tube radius; e and h are defined in figure 6b; and F_e is the force required to fully engage the two tubes. The axial force F_e was experimentally found to be 2,000 lb. Hence, for $R = 2.1$ inches, $e = 3.0$ inches, and $h = 13.0$ inches, equation (7) gives

$$P_{SLIP} = 250 \text{ lb} \tag{8}$$

A precise analysis of the lateral load configuration shown in figure 6b was undertaken, using BOSOR, a well known finite difference computer code for the analysis of shells of revolution (ref. 1). Two cases were analyzed. In the first case the contact regions BC/DE and HI/JK (see fig. 5a) were not allowed any relative motion (i.e., no slip). The ratios P/Δ and P/ϵ were computed to be 22,300 lb/inch and -10,000,000 lb/inch/inch, respectively. For the second case the contact regions were allowed to move relative to each other except for the radial contact deflection. The ratios P/Δ and P/ϵ were found to be 15,000 lb/inch and 1,670,000 lb/inch/inch, respectively. These ratios were then combined with the slip load given by (8) resulting in the analytical prediction of the load cycle 1-2-3-4-5-6-2 shown in figures 7b and 7c. The agreement between experiment and prediction is seen to be reasonably good.

3. Analytical predictions of the allowable moment carrying capability of each of the two joint concepts can be accessed using the following expressions. For joint concept I

$$M_A = \mu R k \delta (1 - \delta/e_o)/(\tan \beta + \mu)/\pi \tag{9}$$

where the various variables are those defined previously in equations (5) and (6). For joint concept II

$$M_A = 2\pi e R t \left(\frac{\lambda t \sigma}{3} - \frac{E \Delta r}{2\lambda R^2} \right) \tag{10}$$

where

$$\lambda^4 = 3(1 - \nu^2)/(R^2 t^2) \tag{11}$$

and where ν is Poisson's ratio, σ is the allowable stress of the tube material, and the remaining variables are as previously defined. Using $R = 2$ inches, $\delta = 0.2$ inch. $\mu = 0.2$, $k = 200,000$ lb/in., $\beta = 1.5$ degrees, $e = 1.5$ inches in equation (9) gives for a feasible type I joint,

$$M_A = 20,000 \text{ in.-lb.}$$

Using $R = 2$ inches, $t = 0.1$ inch, $e = 3$ inches, $E = 30,000,000$ psi. $\nu = 0.3$, $\Delta r = 0.003$ inch, $\sigma = 100,000$ psi in equations (10) and (11) gives, for a feasible type II joint,

$$M_A = 25,000 \text{ in.-lb.}$$

These joint allowables may then be compared with the typical theoretical moment carrying capability given by equation (2).

CONCLUDING REMARKS

This paper presents some of the results of an analytical/experimental evaluation of the behavior of two types of deployable aerospike boom designs. Some useful analytical design procedures have been developed and experimentally verified. Such analytical procedures have provided not only the basis for understanding how each type of boom/joint system functions physically, but also the tools necessary in guiding design changes which have led to the continual improvement of the load carrying capacity of the two types of design concepts.

Because of space limitations the results of many other completed investigations have been omitted. These deal with such topics as the study of the effects of aerodynamic heating upon the boom/joint performance, the dynamic characteristics of each design concept, and the study of the interaction between the boom deployment process and the housing/nose fairing structure.

REFERENCE

1. Bushnell, David:"Analysis of Ring-Stiffened Shells of Revolution Under Combined Thermal and Mechanical Loading," AIAA Jour., vol. 9, No. 3, Mar. 1971, pp. 401-410.
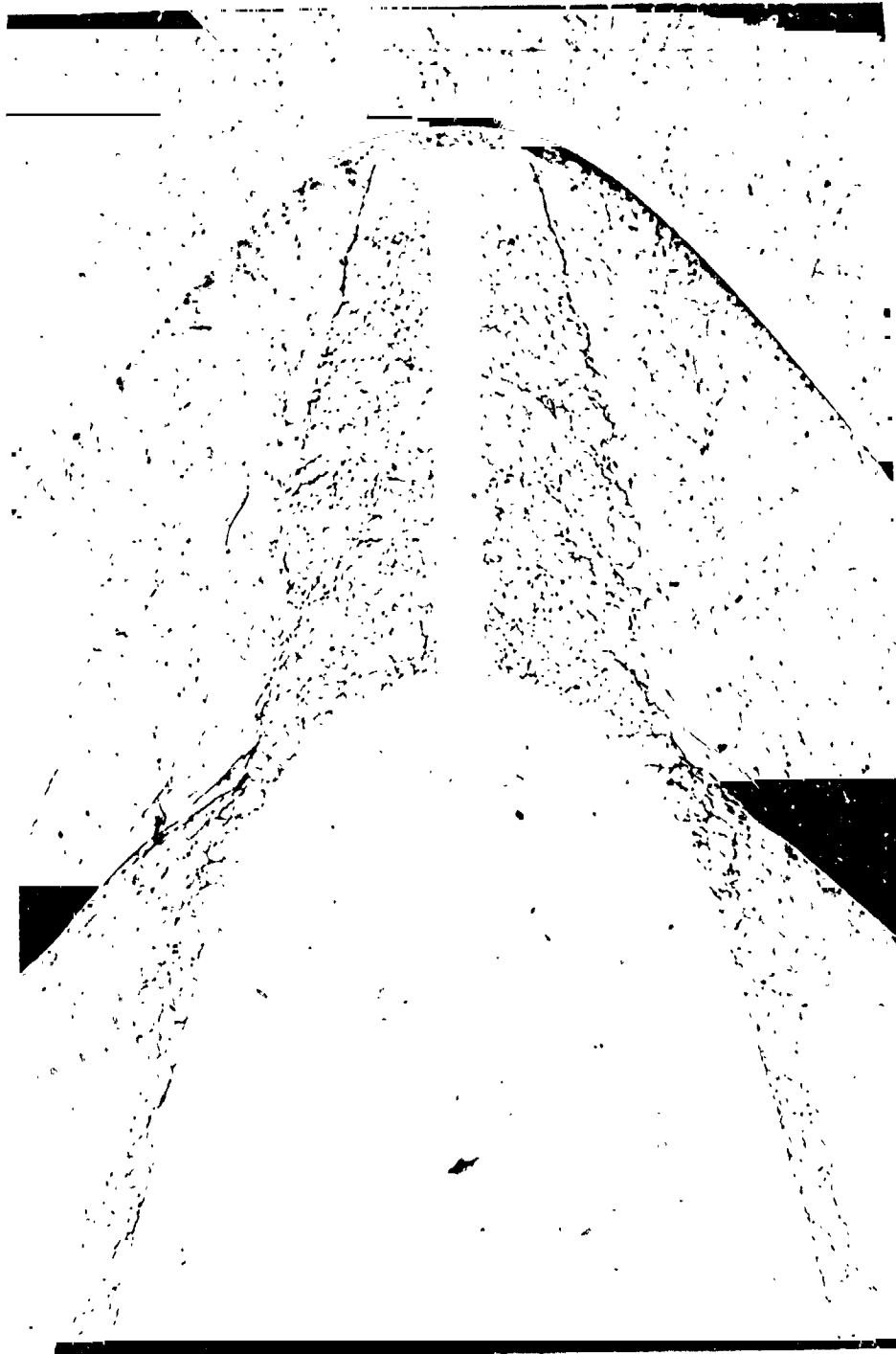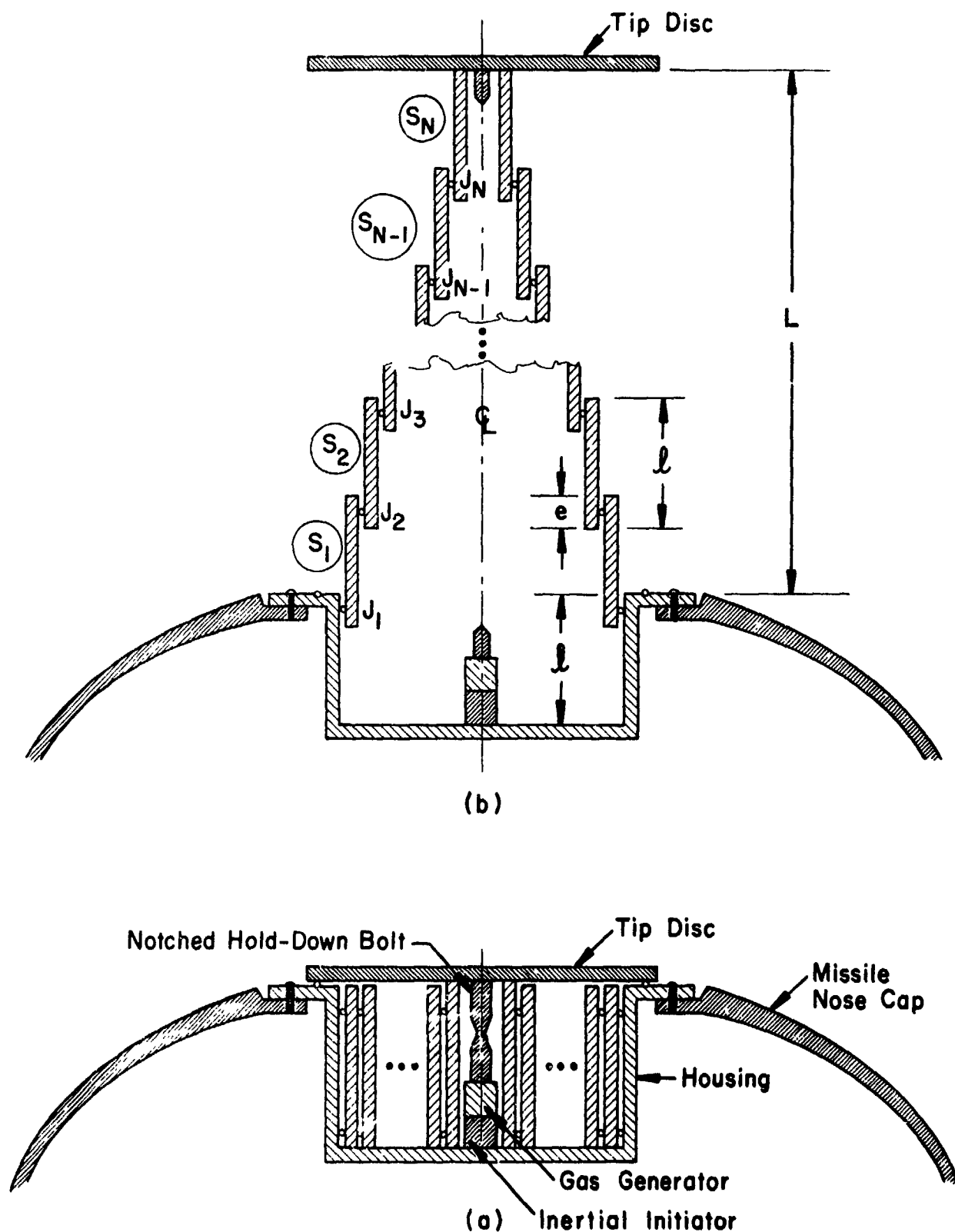
Figure 1. Aerospike-Induced Flow Pattern

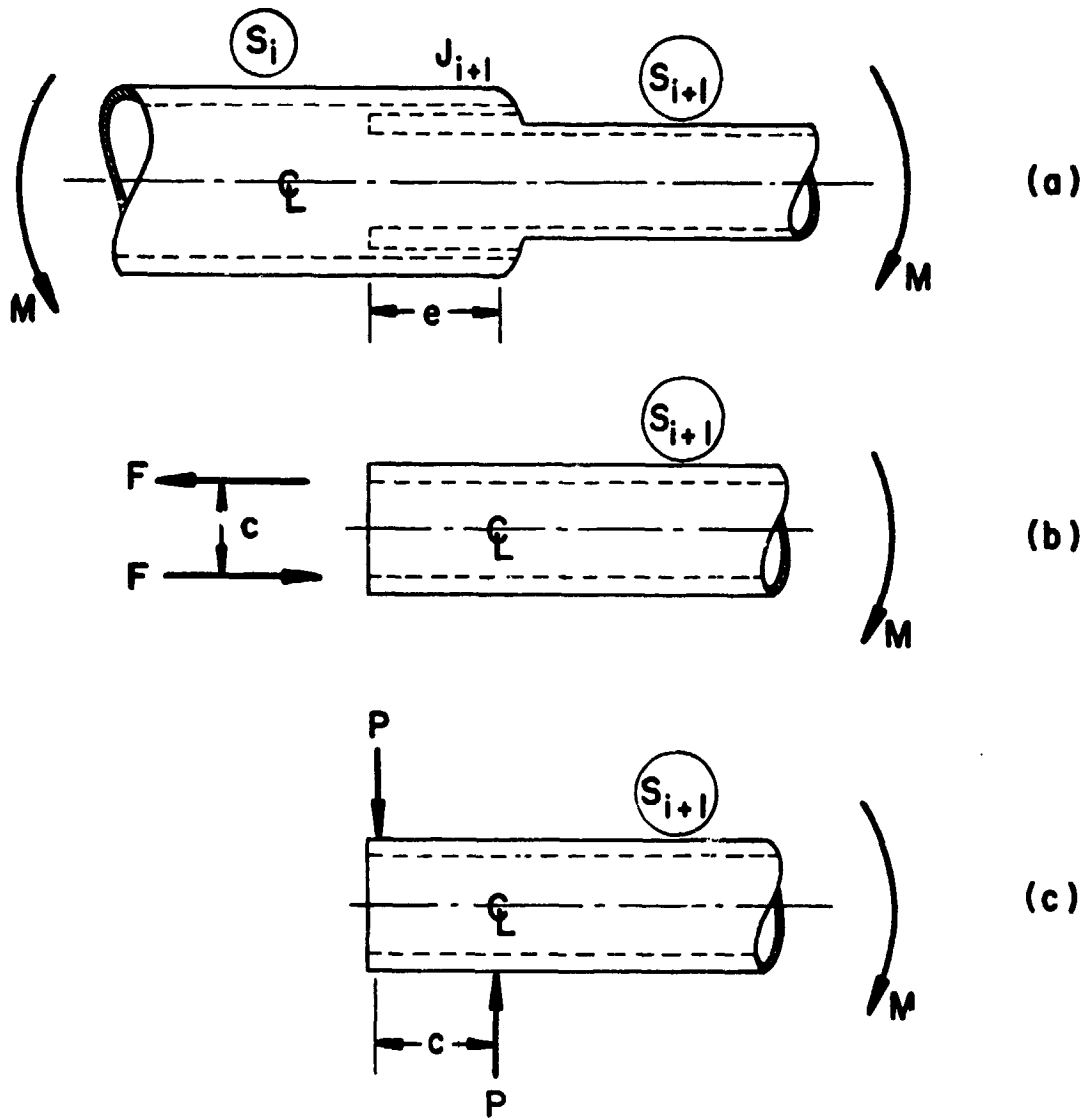Figure 2. — Aerospike configuration (a) stowed, (b) extended.

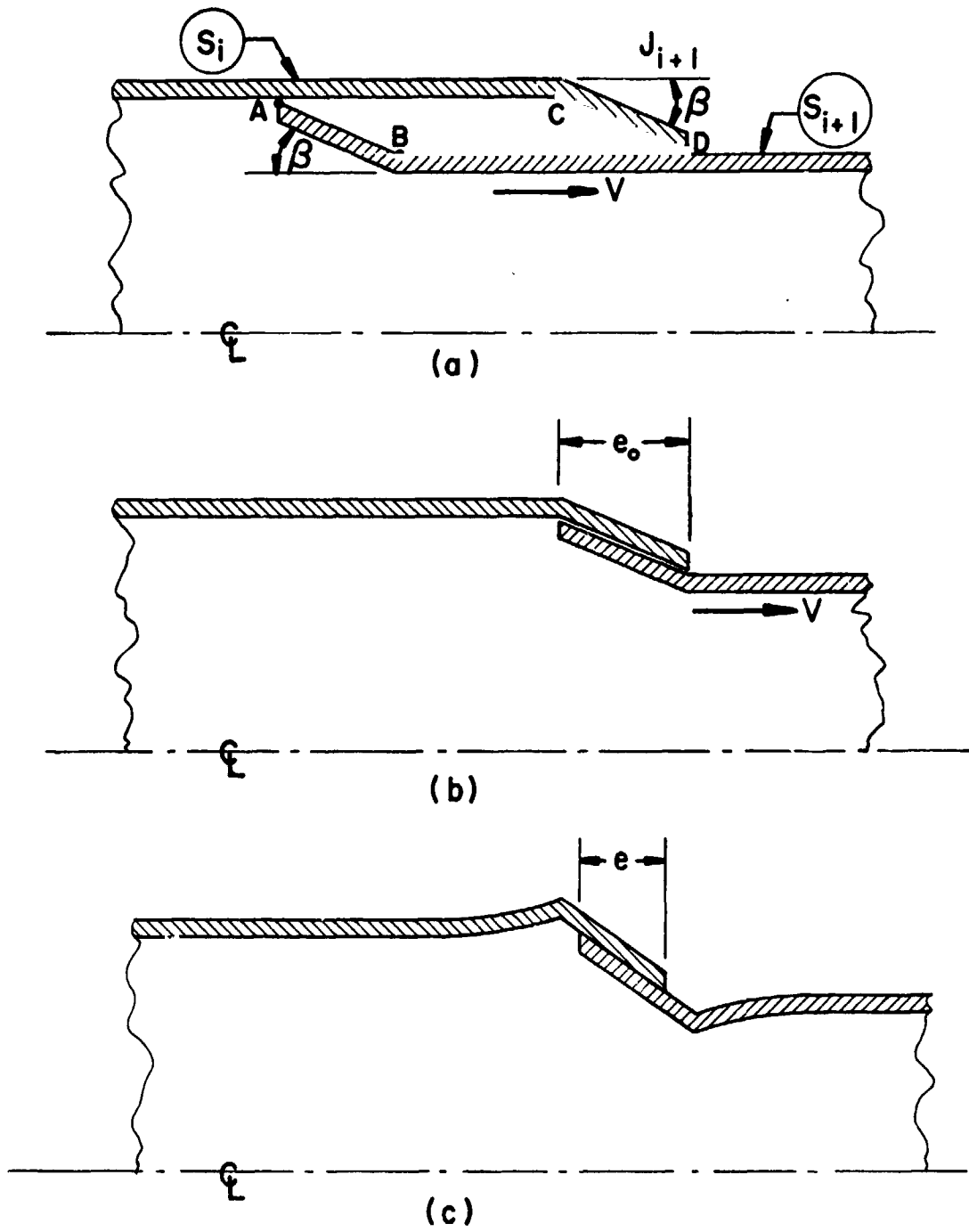Figure 3. — Load carrying characteristics of a typical joint.

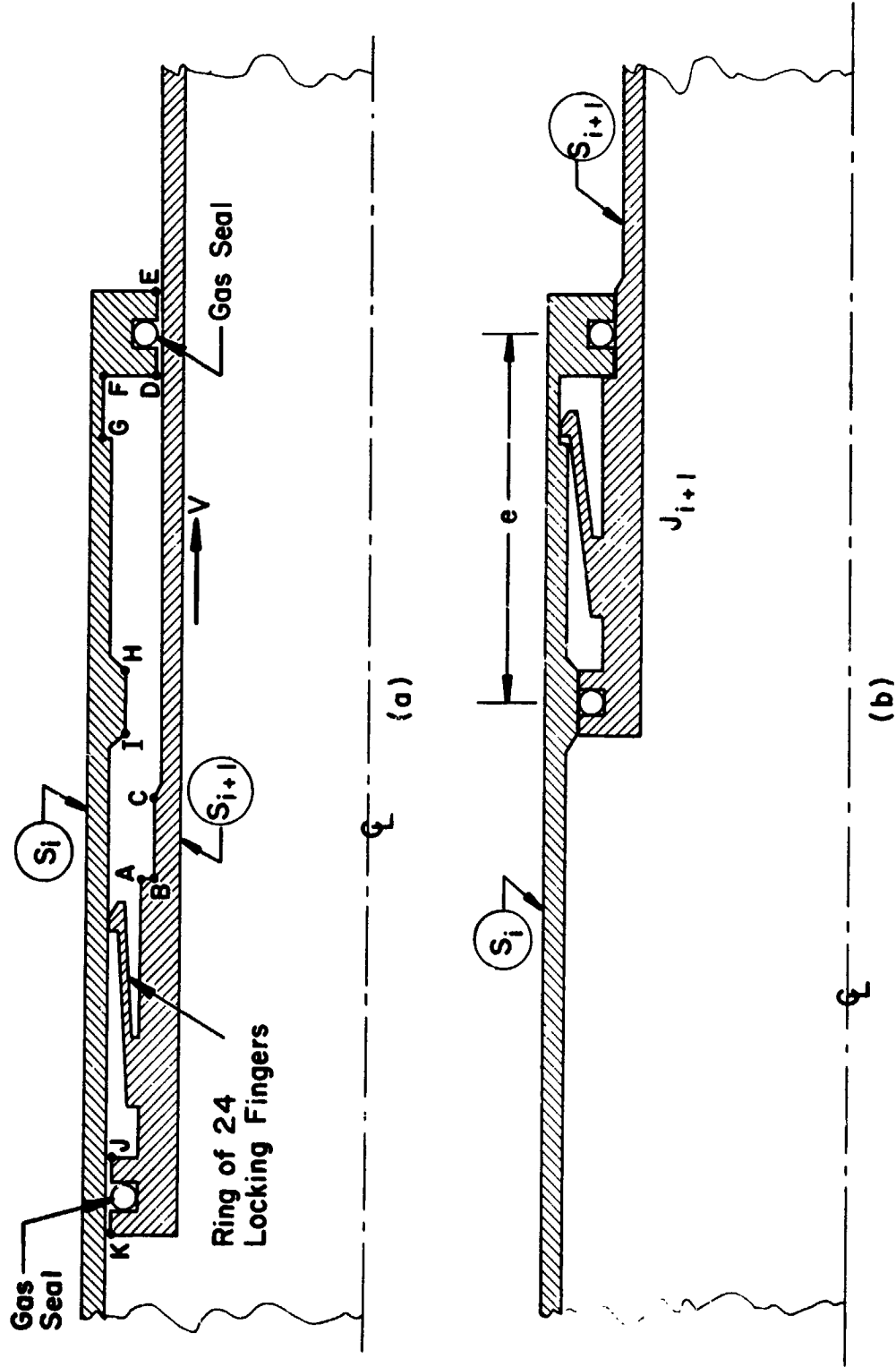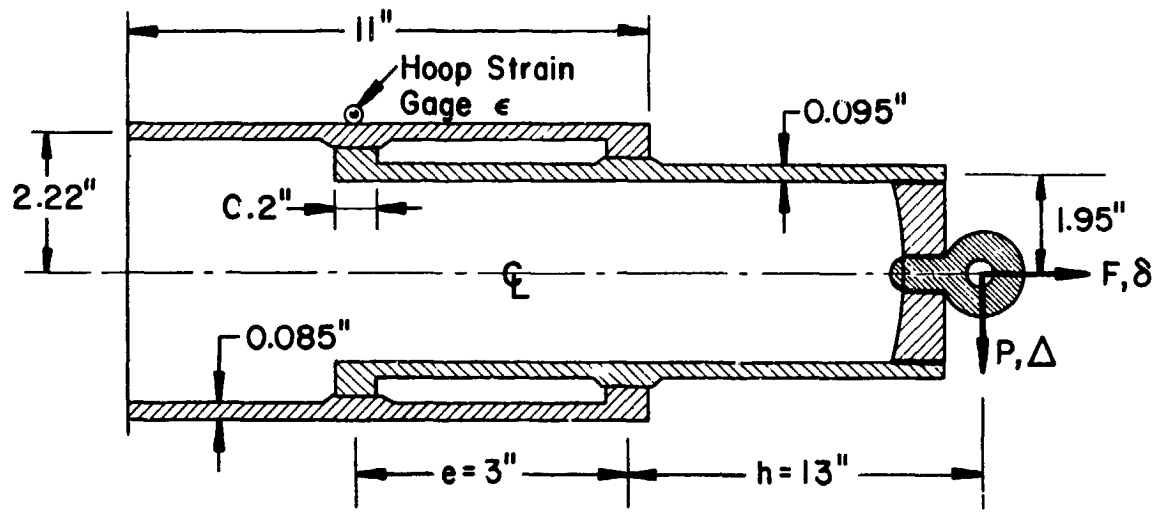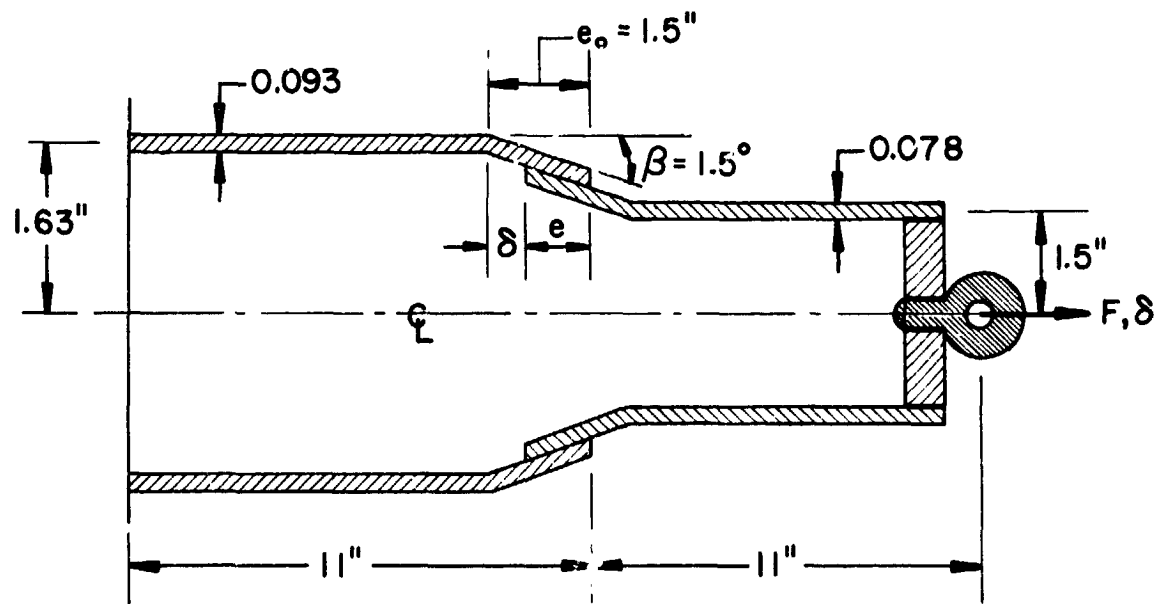Figure 4. — Schematic operation of type I joint.

Figure 5. — Schematic operation of type II joint.
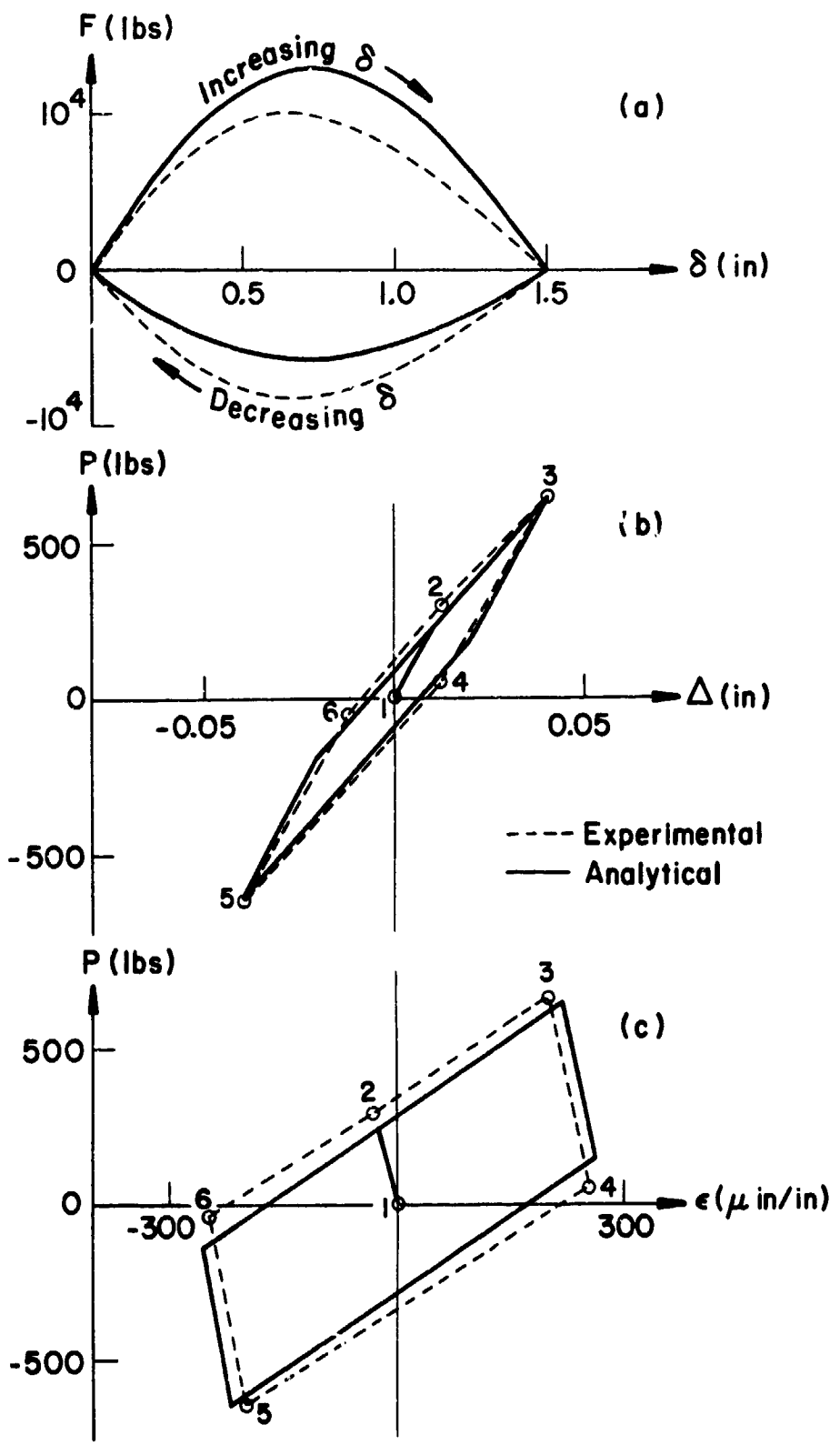
41

Figure 6. — Geometry of joint test specimens.

Figure 7. — Experimental comparison with analyses.